Electronic Supplementary Material (ESI) for Analyst

Supplementary Data

Diffuser-Incorporated Transmission NIR Measurement for Reliable Analysis of Packed Granular Samples

Jihye Yoon,[1] *Jaejin Kim,*[2] *Pham Khac Duy,*[1] *Mooeung Kim*[1] *and Hoeil Chung*[1,*]

[1] Department of Chemistry and Research Institute for Natural Sciences, Hanyang University, Seoul 133-791, Republic of Korea

[2] Jeollanamdo Institute of Natural Resources Research, Jangheung-gun, Jellanamdo, 529-851 Republic of Korea

*Corresponding author

Email: hoeil@hanyang.ac.kr

Tel: 82-2-2220-0937

Fax: 82-2-2299-0762

NIR mapping of a single pellet to investigate internal inhomogeneity

For the investigation of possible internal inhomogeneity inside a pellet, a sectioned sample was prepared by slicing out the middle part of a pellet with a thickness of ~1.0 mm. Diffuse reflectance NIR spectra were then collected along the line of diameter using a NIR microscope with a point-to-point spacing of 45 μm and an aperture of 150 μm. Nearly identical NIR features among the line-mapped spectra would indicate homogeneity inside the pellet. Conversely, internal inhomogeneity would be confirmed if either systematic or discrete spectral variations were observed.

To easily visualize the overall spectral variation across the line mapping, principal component analysis (PCA) was performed using the mapped spectra, and the corresponding score variation (up to fourth scores) was investigated for the high- , middle- and low- density samples. In each case, the score able to show internal inhomogeneity most apparently was selected out of four scores. Figure S-1 (a) shows the variation of second scores across the mapping line for the high-density sample (0.961 $g \cdot cm^{-3}$). As shown, the pattern of score variation is U-shaped, clearly supporting a density gradient between the outside and inside of the pellet. Fig. S-1 (b) and (c) show the variations of the first and fourth scores along the mappings of the middle- (0.934 $g \cdot cm^{-3}$) and low-density (0.918 $g \cdot cm^{-3}$) samples, respectively. For the middle-density pellet, a U-shape pattern was also observed. Although the score variation for the low-density PE was not clearly U-shaped, the density difference between the outer and inner part of the pellet was obvious. The score variations across the mapping lines demonstrated the internal micro-inhomogeneity inside the pellet, as was also confirmed by analysis of micro-sectioned samples from the PE pellet using DSC (differential scanning calorimetry).[1]

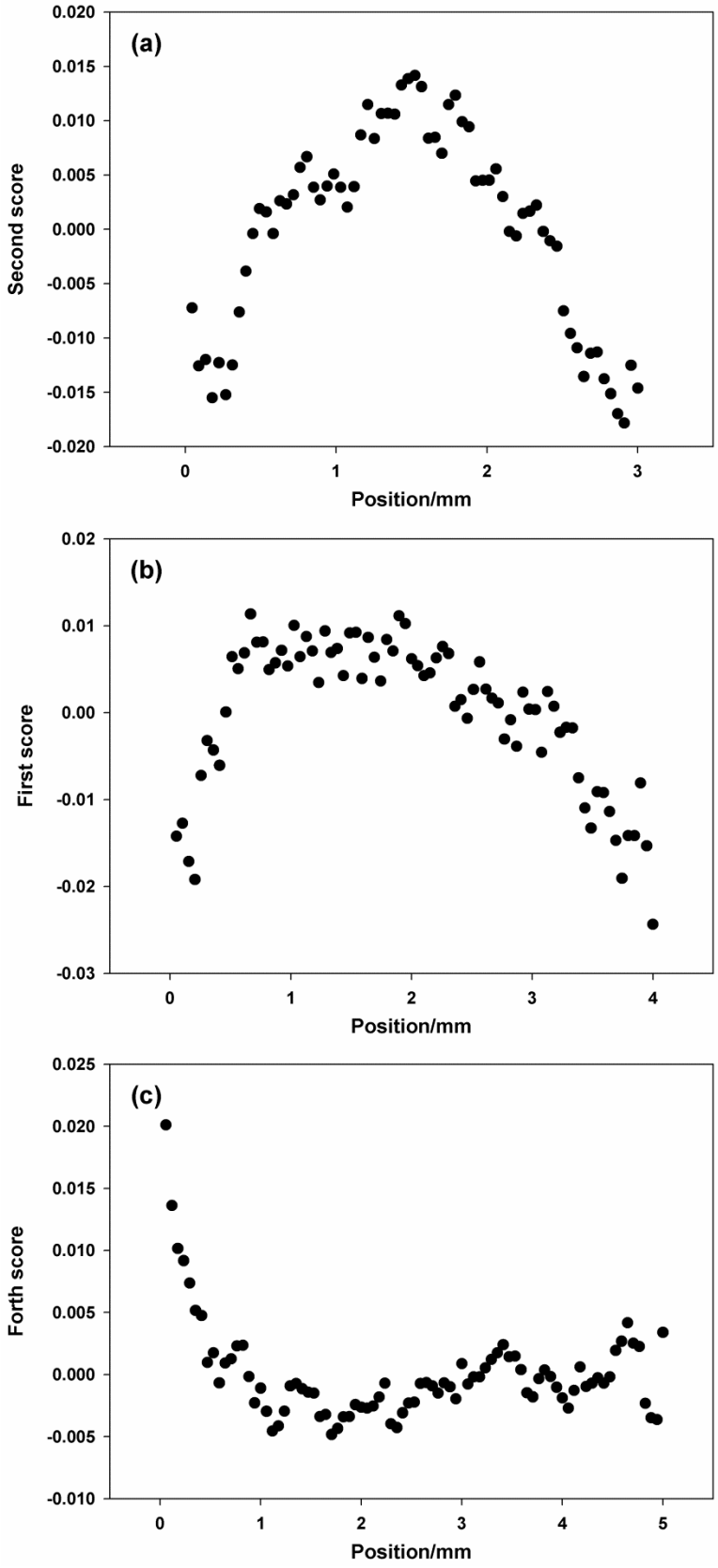

Figure S-1. The score variation across the mapping line acquired from high (a), middle (b), and low density (c) PE pellet.

Three-dimensional score scatter plots used for discrimination of rice samples

Figure S-2 (a) and (b) show three-dimensional score scatter plots providing the best discrimination accuracy for the measurements without and with the diffuser, respectively. White and red circles correspond to Korean and Chinese rice samples, respectively. The plane indicates the boundary of discrimination constructed by LDA. As shown, the separation of two groups is relatively more discernible when the diffuser-incorporated transmission measurement is used.

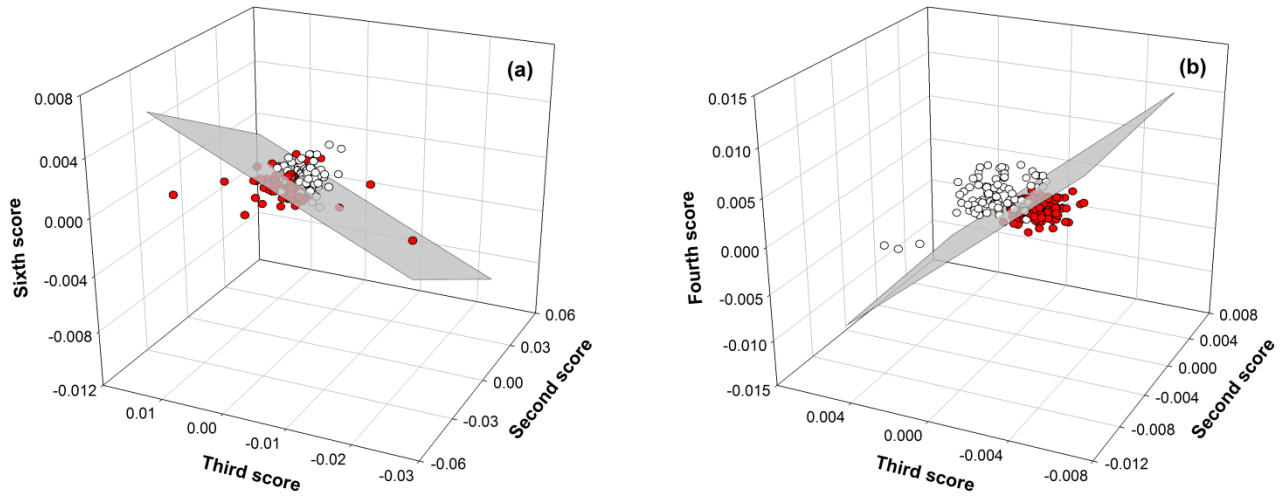

Figure S-2. Three-dimensional score scatter plots showing the best discrimination accuracy from measurements without (a) and with (b) the diffuser, respectively. White and red circles correspond to Korean and Chinese rice samples, respectively. In each plot, the corresponding boundary plane determined by LDA is also shown.

To explain the improved discrimination using the diffuser-incorporated measurement, the spectral differences of rice samples from the two origins were examined. Averages and standard deviations of absorbances at each wavenumber were calculated using spectra belonging to each geographical origin. The average spectra (10600-7700 cm^{-1} range) corresponding to both geographical origins calculated using the spectra collected without and with the diffuser are shown in Figure S-3 (a) and (b), respectively, with the black and red colors denoting Korean and Chinese rice samples, respectively. Average spectra are slightly different in the measurements without the diffuser; while, they are nearly identical with the diffuser-incorporated measurements.

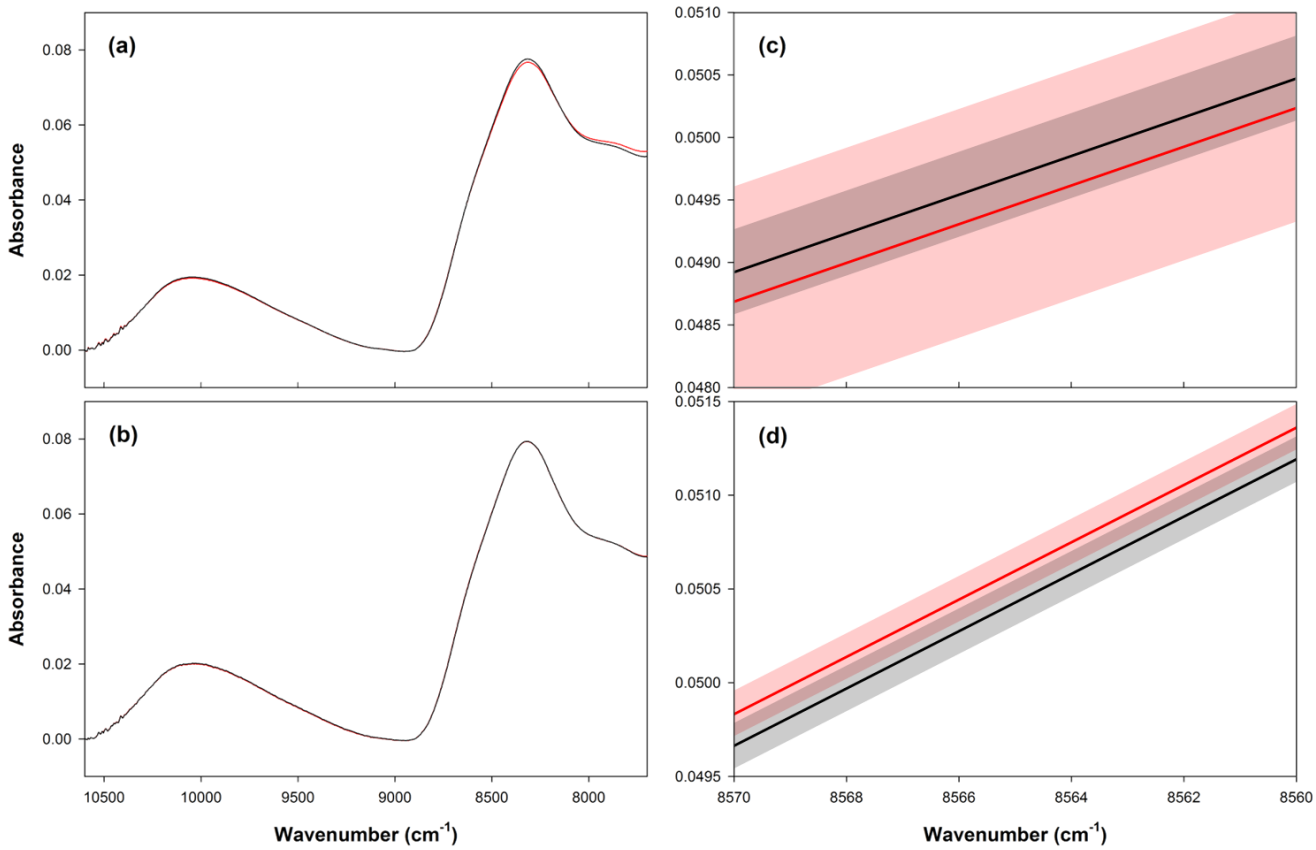

Figure S-3. Average spectra (10600-7700 cm^{-1} range) corresponding to both geographical origins calculated using spectra collected without (a) and with (b) the diffuser. Black and red colors indicate Korean and Chinese rice samples, respectively. The 8570-8560 cm^{-1} range is highlighted for the diffuser-absent (c) and diffuser-incorporated (d) measurements.

For a more detailed analysis, the narrow spectral range from 8570 to 8560 cm^{-1} was highlighted for the diffuser-absent and diffuser-incorporated measurements as shown in Fig. S-3 (c) and (d), respectively. The shades indicate the corresponding standard deviations (1 σ). In the case of diffuser-incorporated measurements, the standard deviations of both geographical origin spectra slightly overlap with each other at a probability of 66.7% (1 σ), while the standard deviations were considerably inter-crossed in the diffuser-absent measurements. The largely overlapped standard deviation in the diffuser-absent measurement mainly came from degraded spectral reproducibility due to NFIR. Thus, the difference in the average spectra of diffuser-absent measurements is relatively more contributed from unsatisfactory reproducibility, along with the differences of sample composition. Obviously, the reproducible spectral features of packed rice samples achieved by the diffuser-incorporated

measurement enabled minute spectral differences to be recognized, which improved the sample discrimination.

Heterogeneous distribution of constituents in a rice grain

To further study the origin of minute spectral differences observed in the average spectra in Fig. S-3 (b), internal inhomogeneity inside a rice grain was also investigated. For this purpose, a rice grain was sectioned such that the inhomogeneous distribution of constituents could be observed. A picture of the sectioned rice grain face is shown in Figure S-4, where the embryo (inside yellowish color) and endosperm (translucent white color) are clearly apparent.

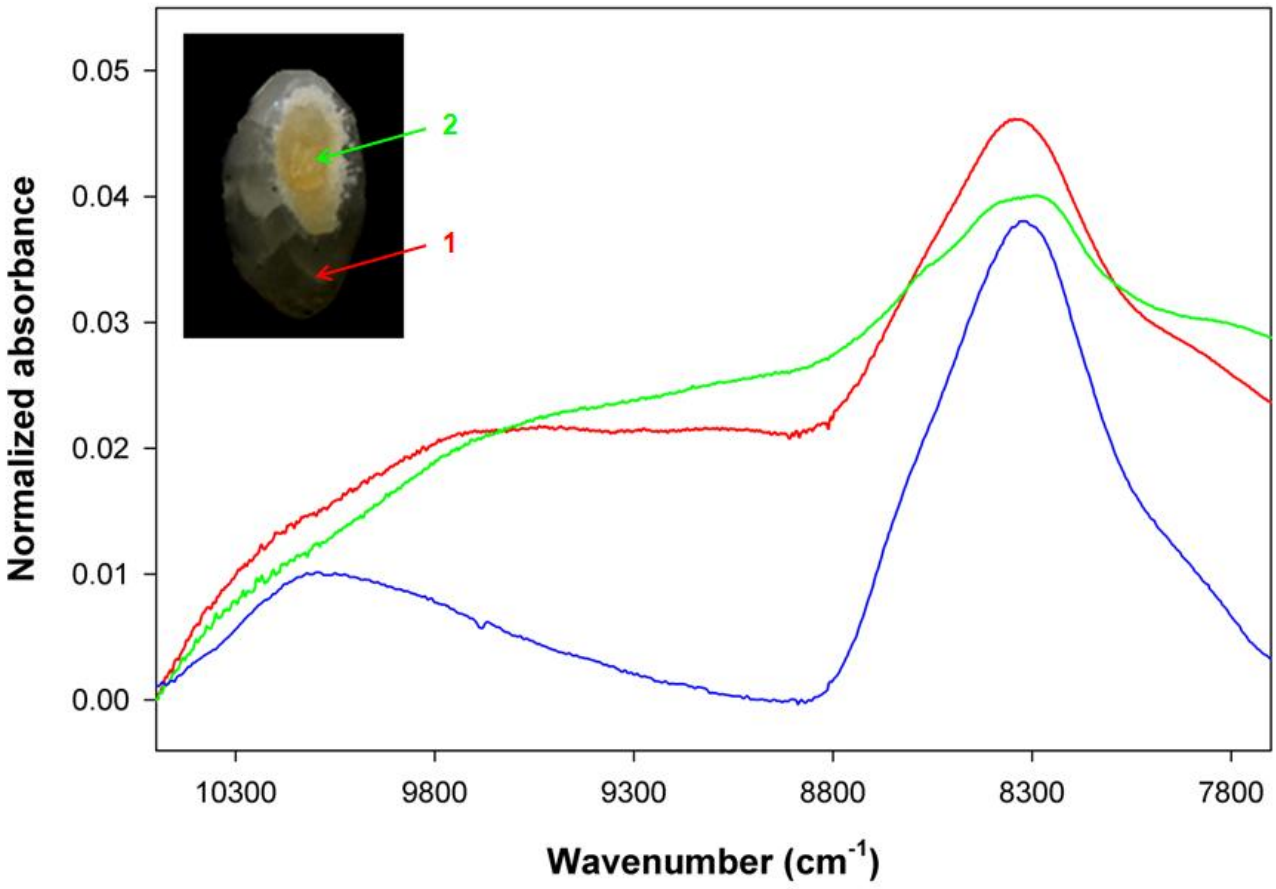

Figure S-4. NIR spectra of the endosperm (1) and embryo (2) as shown in the picture of the sectioned grain face. The arrows indicate the spots where NIR spectra were collected. For comparison, a starch spectrum (blue) is also shown.

Diffuse reflectance NIR spectra collected at 2 different places (indicated by arrows) on the grain face using a microscope (aperture size: 200 μm) are shown in the figure. For comparison, a starch spectrum (blue) is also shown. The spectra are relatively noisy due to decreased light throughput from using a small aperture. The features of spectrum #1 (red) acquired at the endosperm were similar to that of starch, since the endosperm is mostly composed of starch. The features collected at the embryo (#2, green) were largely different from that of endosperm, since the major component in embryo is fat. Minute spectral differences between the two sample groups shown in Fig. S-3 (d) are now explainable as compositional differences of rice constituents such as starch and embryo.

References

1 M. Kim, H. Chung and Y. Jung, J. Raman Spectrosc., 2011, 42, 1967.